BOUNDS ON THE EXISTENCE OF NEUTRON RICH NUCLEI IN NEUTRON STAR INTERIORS*

F. Douchin[a] and P. Haensel[a,b]

[a]Centre de Recherche Astronomique de Lyon
Ecole Normale Supérieure de Lyon
46, allée d'Italie, 69364 Lyon, France

[b]N. Copernicus Astronomical Center
Polish Academy of Sciences
Bartycka 18, 00-716 Warszawa, Poland

(Received July 4, 1998)

We address the question concerning the maximum density, $\rho^{\mathcal{N}}_{\rm max}$, at which nuclei (and more generally — nuclear structures) can exist in neutron star interiors. An absolute upper bound to $\rho^{\mathcal{N}}_{\rm max}$ is obtained using the bulk approximation, in which surface and Coulomb effects are neglected. A very good approximation to $\rho^{\mathcal{N}}_{\rm max}$ is given by the threshold for the instability of a uniform *npe* plasma with respect to density modulations; this threshold is calculated using the Extended Thomas–Fermi approximation for the Skyrme energy functionals. For recent SLy Skyrme forces, which are particularly suitable for the description of very neutron rich nucleon systems, one gets $\rho^{\mathcal{N}}_{\rm max} = 0.08\,{\rm fm}^{-3}$; at this density protons constitute only 4% of nucleons.

PACS numbers: 97.60.Jd, 21.65.+f, 95.30.Cq

1. Introduction

Neutron drip instability limits the neutron excess of neutron-rich nuclei which can be formed in laboratory to $\delta = (N-Z)/A < \delta_{\rm n-drip} \simeq 0.3$. However, this limitation is no longer valid for nuclei in the interiors of neutron stars, where the density varies from a few g cm^{-3} near the stellar surface to more than 10^{15} g cm^{-3} near the star center. Above 10^4 g cm^{-3}, atomic structures are crushed, and electrons form an essentially uniform Fermi gas. Standard scenario of neutron star formation in gravitational collapse of a

* Presented at the International Conference "Nuclear Physics Close to the Barrier", Warszawa, Poland, June 30–July 4, 1998.

massive stellar core (or of a mass accreting white dwarf) predicts nuclear composition corresponding to the state of complete thermodynamic equilibrium (minimum of the free energy per nucleon). Neutron excess parameter of nuclei, immersed in electron gas, increases with increasing density (*i.e.*, increasing depth below stellar surface). Beta decay of neutron rich nuclei, which would be uns in vacuum, is blocked via Pauli exclusion principle due to the presence of dense, degenerate electron gas. Up to the density $4 - 6 \times 10^{11}$ g cm^{-3}, neutron star matter consists of nuclei immersed in dense electron gas. At higher densities, neutrons start to populate continuum states, forming a degenerate neutron gas. The presence of an outer degenerate neutron gas influences the properties of nuclei by: (a) blocking (due to Pauli exclusion principle) neutron emission from nuclei, (b) exerting pressure on nuclei (*i.e.* compressing them), and (c) modifying (lowering) nuclear surface energy.

Further increase of density is accompanied by an increase of the fraction of volume occupied by nuclei and a simultaneous decrease of proton fraction in neutron star matter (and in nuclei). In classical terms, nucleon component of neutron star matter consists there of two coexisting nucleon fluids: denser one in the interior of nuclei, and the less dense outer neutron gas (at highest densities the less dense nucleon fluid can contain some admixture of protons, see Section 2). At some density $\rho_{\rm max}^{\mathcal{N}}$ the two-fluid phase becomes unstable with respect to transition into a uniform, electrically neutral *npe* plasma, composed mostly of neutrons, with a few percent admixture of electrons and protons. The density $\rho_{\rm max}^{\mathcal{N}}$ is the maximum density, at which nuclei can exist in the neutron star interiors; it turns out to be significantly lower than normal nuclear saturation density $\rho_0 = 0.16$ fm^{-3}, typically $\sim \frac{1}{2}\rho_0$ (see Section 3). Before $\rho_{\rm max}^{\mathcal{N}}$ is reached, the interplay between Coulomb and surface effects can lead to the appearance of unusual shapes of 'nuclei' (rods, plates, tubes, bubbles, ...). However, both the theoretical value of $\rho_{\rm max}^{\mathcal{N}}$ and the actual shape of 'nuclei' (the more appropriate term would be 'nuclear structures') at highest densities, depend on the assumed effective nuclear hamiltonian, used in many-body calculations [5,6,8,9,11]. For some effective N–N interactions, neutron star matter contained spherical nuclei down to $\rho_{\rm max}^{\mathcal{N}}$ (SkM force in [9], all relativistic mean field models in [5]). For other models of effective N–N forces, spherical nuclei were replaced by a sequence of cylindrical ones (rods), flat (plates), cylindrical holes in nuclear matter filled by neutron gas (tubes), and finally spherical holes in nuclear matter filled by neutron gas (bubbles), before disappearance of nuclear structures at $\rho_{\rm max}^{\mathcal{N}}$ [6,8,9,11].

Let us stress that up to about ρ_0 the elementary constituents of neutron star matter are still the same as those of terrestrial matter: n, p, e (see, *e.g.*, [13]). However, under extremal conditions prevailing in neutron star

interior, the *structures* these constituents form can be dramatically different from those familiar from terrestrial ones.

The quantity $\rho_{\max}^{\mathcal{N}}$ has an important astrophysical meaning: it determines the bottom boundary of the neutron star *crust*, an outer envelope, in which nuclei form a periodic crystal lattice due to longer range Coulomb interactions. In the case of unusual nuclei, one deals rather with two dimensional (rods, tubes) or even one dimensional (plates) liquid crystals [6–9]. The solid crust plays an important role in the evolution and dynamics of neutron stars (see, *e.g.* [13]).

In view of the fact, that the bottom layers of neutron star crust involve nucleon matter with an extremely large neutron excess ($\delta \simeq 0.9$), an appropriate choice of effective nuclear hamiltonian is of crucial importance. Recently, a new set of the Skyrme-type effective N–N interactions SLy (Skyrme Lyon) has been derived, based on an approach which is particularly appropriate, as far as the applications to a neutron rich matter are concerned [3,4]. Relevant additional experimental items concerning nuclei with large neutron excess, isovector effective masses, constraints of spin stability, and requirement of consistency with the realistic UV14+VIII equation of state (EOS) of dense neutron matter of Wiringa *et al.* [14] for $\rho_0 \leq \rho \leq 1.5$ fm^{-3}, were included into a fitting procedure for the SLy forces parameters. In the present paper we calculate $\rho_{\max}^{\mathcal{N}}$ using the SLy models of effective N–N interaction, and compare our results with those obtained using older Skyrme-type forces, Sk1′ and SkM*, used frequently in astrophysical applications. The parameters of the SLy forces, used in the present calculations, together with those of the SkM* and Sk1′ models, are given in Table I. The SLy4 is a basic SLy force; the SLy7 model has been obtained following the most ambitious fitting procedure, in which spin-gradient terms and center of mass correction term were both included in the Skyrme energy functional [4].

At the densities of interest, matter in the interior of a neutron star which is more than one year old, is strongly degenerate, and thermal contributions to thermodynamic quantities can be safely neglected. In what follows, we will consider the properties of neutron star matter in the $T = 0$ approximation; dense matter will be assumed to be in its ground state (it is then called 'cold catalyzed matter').

In Section 2, we present the calculation of $\rho_{\max}^{\mathcal{N}}$ in the bulk approximation. Threshold for the instability of homogeneous *npe* matter with respect to density modulations (*i.e.*, formation of 'nuclear structures') is calculated in Section 3. Properties of very neutron rich nuclei in the bottom layers of neutron star crust, and dependence on the effective N-N interaction model, are discussed in Section 4. Concluding remarks are presented in Section 5.

TABLE I

Parameter values of the Skyrme forces

Force	SLy4	SLy7	SkM*	Sk1′
t_0 (MeV fm^3)	-2488.91	-2482.41	-2645.0	-1057.3
t_1 (MeV fm^5)	486.82	457.97	410.0	235.9
t_2 (MeV fm^5)	-546.39	-419.85	-135.0	-100.00
t_3 (MeV fm$^{3+3\sigma}$)	13777.0	13677.0	15595.0	14463.5
σ	$\frac{1}{6}$	$\frac{1}{6}$	$\frac{1}{6}$	1
x_0	0.834	0.846	0.09	0.2885
x_1	-0.344	-0.511	0	0
x_2	-1.000	-1.000	-1.000	0
x_3	1.354	1.391	0	0.2257
W_0 (MeV fm^5)	123.0	126.0	130.0	120.0

2. Bound for the existence of nuclei: the bulk approximation

Above neutron drip density, $\rho_{\mathrm{n-drip}}$, neutron star crust is a two-phase nucleon system, the denser nucleon phase (fluid) 'i' residing inside nuclei and the less dense 'o' one forming a gas outside nuclei. Both nucleon fluids are permeated by an essentially homogeneous electron gas, which ensures overall charge neutrality. The shape of nuclei, *i.e.* that of the 'i-o' interface, results from the balance of the surface and Coulomb terms in the total energy of the system.

The bulk approximation consists in neglecting the Coulomb and surface effects. At given mean nucleon density ρ, nucleons are present in general in both of the coexisting 'i' and 'o' fluids, characterized by the constant densities $\rho_{n\mathrm{i}}$, $\rho_{p\mathrm{i}}$, $\rho_{n\mathrm{o}}$, and above proton drip density, $\rho_{\mathrm{p-drip}}$, also $\rho_{p\mathrm{o}}$. The equilibrium between the 'i' and 'o' fluids, ensured by the (strong) N–N interaction, implies the equality of the chemical potentials of nucleons, and the equality of nucleon pressures,

$$\mu_{n\mathrm{i}} = \mu_{n\mathrm{o}}, \qquad \mu_{p\mathrm{i}} = \mu_{p\mathrm{o}}\ , \qquad P_{N\mathrm{i}} = P_{N\mathrm{o}}\ , \tag{1}$$

where the label N indicates the nucleon contribution to the matter pressure, and the condition on the proton chemical potentials applies only above the proton-drip density, $\rho_{\mathrm{p-drip}}$. At a given ρ, Eqs. (1) enables determination of $\rho_{n\mathrm{i}}$, $\rho_{p\mathrm{i}}$, $\rho_{n\mathrm{o}}$, and for $\rho > \rho_{\mathrm{p-drip}}$, also $\rho_{p\mathrm{o}}$.

Let us denote the volume fraction occupied by the 'i' fluid by u. At a given mean nucleon density $\rho = u\rho_{\mathrm{i}} + (1-u)\rho_{\mathrm{o}}$, the total energy density is

given by

$$E = uE_{N\mathrm{i}} + (1-u)E_{N\mathrm{o}} + E_e \ , \tag{2}$$

where E_e is the electron energy density, $E_e(\rho_e)$. Beta equilibrium within the *npe* matter implies relation between the chemical potentials of neutrons, protons and electrons,

$$\mu_n = \mu_p + \mu_e \ , \tag{3}$$

while requirement of the overall charge neutrality leads to

$$\rho_e = u\rho_{p\mathrm{i}} + (1-u)\rho_{p\mathrm{o}} \ . \tag{4}$$

Eqs. (1), (3), (4) determine completely the equilibrium of a two-fluid *npe* matter at a given nucleon density ρ.

The two-fluid phase is stable at a given ρ if its energy per nucleon is lower than that in the uniform (one-fluid) phase (*i.e.*, that of a uniform *npe* matter). This stability condition breaks down at a density $\rho_{2\leftrightarrow 1}$. Calculations show that approaching $\rho_{2\leftrightarrow 1}$ from the lower density (two-fluid)

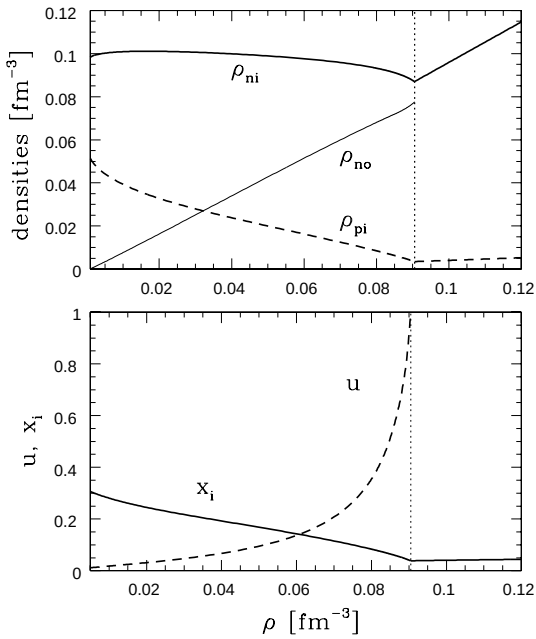

Fig. 1. Composition and the two-fluid–one-fluid phase transition in the bulk approximation, for the SLy4 force. Two-fluid phase to the left, one-fluid phase to the right of the dotted line representing the bottom boundary of the crust in the bulk approximation.

TABLE II

Neutron drip and proton drip densities, and proton fraction and nucleon density at the 2-fluid↔1-fluid transition, calculated in the bulk approximation.

Force	$\rho_{n-\mathrm{drip}}$ (fm^{-3})	$\rho_{p-\mathrm{drip}}$ (fm^{-3})	$\rho_{2\leftrightarrow 1}$ (fm^{-3})	$x_{2\leftrightarrow 1}$ (%)
SkM*	7.55×10^{-4}	0.0781	0.0866	3.13
Sk1′	8.09×10^{-4}	0.1066	0.1088	3.71
SLy4	7.34×10^{-4}	0.0853	0.0905	3.84
SLy7	7.21×10^{-4}	0.0836	0.0889	3.80

side corresponds to $u \longrightarrow 1$, *i.e.* to the 'i' (denser) fluid filling the whole volume [10].

Therefore the $2 \leftrightarrow 1$ transition is a continuous one, with no density jump (our results for the SLy4 force are shown in Fig. 1). Actually, Coulomb and surface effects would increase the energy per nucleon in the two-fluid phase, as compared to the plain bulk approximation. Therefore, the real transition into a uniform *npe* matter occurs at density lower than $\rho_{2\leftrightarrow 1}$, so that $\rho_{2\leftrightarrow 1}$ is thus a robust *upper bound* to $\rho^{\mathcal{N}}_{\max}$.

Numerical values of $\rho_{2\leftrightarrow 1}$ for four Skyrme forces are shown in Table II, where we show also the proton-drip densities, and the proton fractions at the $2 \leftrightarrow 1$ transition point, $x_{2\leftrightarrow 1}$ (bulk instability of two-fluid phase with Skyrme forces SkM and Sk1′ was studied in [10]). As far as the value of $\rho_{2\leftrightarrow 1}$ is concerned, both SLy models yield values close to 0.09 fm^{-3}, intermediate between those corresponding to the Sk1′ and SkM* forces, which yield 0.11 fm^{-3} and 0.087 fm^{-3}, respectively. Proton drip takes place in a narrow interval of densities close to $\rho_{2\leftrightarrow 1}$. At the $2 \leftrightarrow 1$ transition point, protons constitute less than 4% of nucleons.

3. Instability of a uniform *npe* matter and existence of nuclear structures

An instability of a spatially uniform state of the *npe* matter with respect to density modulations signals the appearance of nuclear structures in the true ground state of the *npe* system. Let us consider first a *npe* matter at nucleon density $\rho > \rho_0$, which is sufficiently high to exclude any possibility of

existence of nuclear structures. By decreasing ρ, we will eventually find the threshold density, below which uniform *npe* matter is unstable with respect to density modulations. This threshold density turns out a lower bound (and a rather good approximation) to $\rho^{\mathcal{N}}_{\max}$ [8, 10].

The ground state of uniform *npe* matter of a given nucleon density ρ corresponds to the minimum of the energy density $E(\rho_n, \rho_p, \rho_e) = E_0$, calculated at a fixed nucleon density $\rho = \rho_p + \rho_n = \rho$, under the condition of charge neutrality $\rho_e = \rho_p$ (all densities being *assumed* constant in space). Minimisation implies the beta equilibrium relation between the chemical potentials of matter constituents, $\mu_n = \mu_p + \mu_e$. This relation ensures vanishing of the first variation of E implied by small perturbations $\delta\rho_j(\boldsymbol{r})$ (where $j = n, p, e$). However, this does not guarantee the *stability* of the spatially homogeneous state of the *npe* matter, which requires that the second variation of E (quadratic in $\delta\rho_j$) be positive.

The energy per unit volume, E, of a slightly nonuniform *npe* matter, can be decomposed into nucleon, electron, and Coulomb components,

$$E = E_N + E_e + E_{\rm Coul} \ . \tag{5}$$

The nucleon contribution to E can be expressed in terms of the energy density

$$\mathcal{E}_N(\rho_n, \rho_p, \nabla\rho_n, \nabla\rho_p) \, ,$$

obtained from the Skyrme models of the effective nucleon hamiltonian, so that for a perturbed, slightly spatially inhomogeneous state we get the energy functional

$$E_N = \frac{1}{V} \int {\rm d}\boldsymbol{r} \mathcal{E}_N[\rho_n(\boldsymbol{r}), \rho_p(\boldsymbol{r}), \nabla\rho_n(\boldsymbol{r}), \nabla\rho_p(\boldsymbol{r})] \ . \tag{6}$$

The expression for $\mathcal{E}_N$ has been calculated using the semi-classical Extended Thomas–Fermi (ETF) treatment of the kinetic and the spin-orbit energy densities [2]. Assuming that the spatial gradients are small, one keeps only the quadratic gradient terms in the ETF expressions. This approximation will be justified by the fact that characteristic wavelengths of perturbations turn out to be much larger than the internucleon distance (see below). With such approximations, the change of the energy (per unit volume) implied by the density perturbations can be expressed, keeping only second order terms, as [1, 10],

$$E - E_0 = \frac{1}{2} \int \frac{{\rm d}\boldsymbol{q}}{(2\pi)^3} F_{ij}(\boldsymbol{q}) \delta\rho_i(\boldsymbol{q}) \delta\rho_j(\boldsymbol{q})^* \ , \tag{7}$$

where Fourier representation

$$\delta\rho_j(\boldsymbol{r}) = \int \frac{{\rm d}\boldsymbol{q}}{(2\pi)^3} \delta\rho_j(\boldsymbol{q}) {\rm e}^{{\rm i}\boldsymbol{q}\boldsymbol{r}} \ . \tag{8}$$

has been used. The hermitian $F_{ij}(\boldsymbol{q})$ matrix determines the stability of the uniform state of equilibrium of the *npe* matter with respect to the spatially periodic perturbations of the densities of wavevector $\boldsymbol{q}$. Due to the isotropy of the homogeneous equilibrium state of the *npe* matter, F_{ij} depends only on $|\boldsymbol{q}| = q$. In the case of Skyrme forces, the matrix elements F_{ij} can be calculated analytically, as explicit functions of the equilibrium densities and q, and are composed of compression (local), curvature (gradient), and Coulomb components [1, 10].

The condition for the F_{ij} matrix to be positive definite turns out to be equivalent to the requirement that the determinant of the F_{ij} matrix be positive [9]. At each density ρ, one has thus to check the condition $\det[F_{ij}(q)] > 0$. Let us start with some $\rho > \rho_0$, at which $\det[F_{ij}(q)] > 0$ for any q. By decreasing ρ, we find eventually a wavenumber Q at which stability condition is violated for the first time; this happens at some density $\rho(Q)$. For $\rho < \rho(Q)$ homogeneous state is no longer the true ground state of the *npe* matter since it is unstable with respect to small periodic density modulations.

In contrast to the bulk approximation, in which constant densities were assumed *by construction*, the general energy functional used in this section allows for a consistent treatment of spatially inhomogeneous states of the *npe* matter. The instability at $\rho(Q)$ signals a phase transition with a loss of translational symmetry of the *npe* matter. In principle, this could be a second order phase transition. However, the combination of Coulomb and surface effects turns out to be sufficiently strong to destabilize the *npe* state with an infinitesimal density modulation, leading to a first-order phase transition into a state with finite amplitude density modulations. The real equilibrium phase transition (at constant pressure) will thus take place at a *npe* matter density ρ_1, slightly higher than $\rho(Q)$. Homogeneous *npe* matter of density ρ_1 coexists with a spatially inhomogeneous phase exhibiting some nuclear structures, of a density ρ_2 slightly lower than ρ_1. Therefore, $\rho(Q)$ is actually a *lower bound* on ρ_1, but in view of the closeness of ρ_1 and ρ_2, it can be used as a rather good approximation of $\rho_{\max}^{\mathcal{N}} = \rho_2$.

Our numerical results for four Skyrme forces are shown in Table III ([12], the case of Sk1′ force was studied previously, using slightly different approximations, in [10]). Column "a" was obtained using standard TF approximation to nucleon kinetic energy densities, and neglecting spin-orbit contribution to $\mathcal{E}_N$. Adding quadratic gradient terms in the ETF expansion of the nucleon energy densities [2] (columns "b") increased only slightly the values of $\rho(Q)$ (by less than 1%) as compared to the TF values. Notice that both "a" and "b" were obtained neglecting the spin-orbit term in $\mathcal{E}_N$. Finally, adding the spin-orbit term, calculated using the ETF approximation [2] (column "c"), further increased $\rho(Q)$ by about 1% with respect to the

TABLE III

Threshold for the instability of the homogeneous *npe* matter with respect to density modulations.

Force	$\rho(Q)$ (fm^{-3})			Q (fm^{-1})			$x(Q)$ (%)
	a	b	c	a	b	c	c
SkM*	0.0738	0.0744	0.0754	0.277	0.284	0.299	2.79
Sk1′	0.0992	0.0993	0.1005	0.314	0.319	0.367	3.52
SLy4	0.0781	0.0787	0.0794	0.262	0.271	0.281	3.57
SLy7	0.0773	0.780	0.0786	0.270	0.280	0.292	3.55

a: TF approximation without spin-orbit term.
b: ETF without spin-orbit term.
c: ETF including spin-orbit term.

"b" ones (from 0.8% for SLy7 to 1.5% for Sk1′). In the case of the critical wavenumber Q, corresponding effects are significantly higher.

For the ETF approximation to be correct, the value of the characteristic wavelength of critical density perturbations, $2\pi/Q$, must be significantly larger than the mean internucleon distance. Despite a small proton fraction, $2\pi/Q \sim 17 - 22$ fm is typically four times higher than the distance between protons $r_{pp} = (4\pi\rho/3)^{-1/3}$; for neutrons this ratio is typically about eight.

4. Nuclei in the bottom layers of the crust

The actual structure of the bottom layer of neutron star crust should be calculated including Coulomb and surface effects. One usually considers a limited set of five possible nuclear shapes: spheres of i-phase embedded in o-gas, rods of i-phase in o-gas, equidistant plates of i-phase with o-gas between them, tubes in the i-matter filled with o-gas, and spherical bubbles of the o-gas in i-matter. For a given nuclear shape, the ground state of the matter is calculated using the Wigner–Seitz approximation, in which the real system is replaced by a set of non-interacting, electrically neutral cells, each cell containing one nucleus. Wigner–Seitz cells are spherical, cylindrical or plate-like, depending on the symmetry of nuclear structure. The total volume of cells is equal to the volume of the real system.

By comparing the enthalpies per nucleon $(E+P)/\rho$ at given P, one finds the actual shape of nuclei at this pressure P. Depending on the assumed effective N–N interaction, unusual nuclear shapes (starting with rods) may appear as early as at $\rho \simeq 5 - 6 \times 10^{-2}$ fm^{-3} (the case of FPS force of [9, 6, 11]), or do not appear at all, spherical nuclei being present down to ρ_2 (SkM force case of [9, 5]). Elementary considerations within the liquid drop model indicate, that at lower densities spherical shape is the only possible one. A possibility (or rather a necessity) of appearance of unusual nuclear shapes at highest densities results from the fact, that the fraction occupied by i-phase (*i.e.*, nuclear matter), u, increases with increasing ρ, and above some limiting density the sum of the surface and Coulomb energies can be reduced by changing nuclear shape from spherical to an unusual one. The main point is whether unusual shape will appear *before* the transition into a homogeneous *npe* matter.

In general, the structure of the bottom layers of the neutron star crust may be expected to be rather sensitive to the behavior of the nuclear surface tension, σ, in the relevant density interval $\frac{1}{3}\rho_0 < \rho < \frac{2}{3}\rho_0$. Our results obtained within the ETF approximation for the Skyrme energy functional, shown in Fig. 2 [15], visualize strong dependence of σ at large neutron excess on the Skyrme force used [notice that all these forces lead to very similar values of $\sigma(\delta_{\rm i} = 0)$, consistent with experimental value extracted from the liquid droplet model]. At $\delta_{\rm i} = 0.8$ (which corresponds to the proton fraction

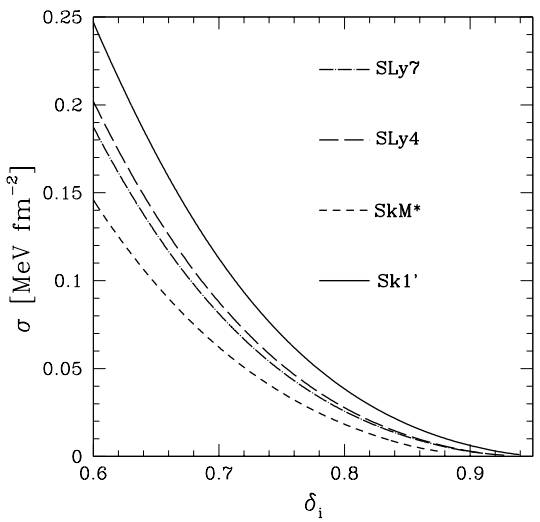

Fig. 2. Surface tension of the i-o phase interface versus neutron excess parameter $\delta_{\rm i} = 1 - 2x_{\rm i}$ in the denser (i) phase far from the interface. Typical values of $\delta_{\rm i}$ ($x_{\rm i}$) range from 0.6 (0.2) at $\rho = 0.05$ fm^{-3} to 0.8 (0.1) at $\rho = 0.08$ fm^{-3}.

$x_{\rm i} = 0.1$), characteristic of $\rho \simeq 0.08$ fm^{-3}, nuclear surface tension for SkM* model is only half of that obtained for the Sk1$'$ one, which in turn is 30% higher than our values for the SLy forces. We should remind, however, that even at $\rho \simeq \frac{1}{3}\rho_0$ we have to deal with nuclei which are very far from the most neutron rich nuclei available in terrestrial nuclear physics, and therefore we should rely on the extrapolation of nuclear models to very high neutron excess. This may be visualized by our preliminary results obtained within the compressible liquid drop model for SLy4 force, shown in Table IV.

TABLE IV

Examples of spherical nuclei in the bottom layers of neutron star crust with SLy4 force. Curvature corrections to surface energy are neglected. $A_{\rm cell}$ is the number of nucleons in Wigner–Seitz cell, u is the fraction of volume occupied by protons, Z and A are numbers of protons and nucleons in nuclei, R_n, R_p are corresponding (equivalent) radii.

ρ (fm^{-3})	$\rho_{\rm o}/\rho_{\rm i}$	u	R_p (fm)	$R_n - R_p$ (fm)	Z	A	$A_{\rm cell}$
0.0160	0.0932	0.0154	5.56	0.83	28.2	133.2	751.3
0.0425	0.2819	0.0551	6.20	0.86	25.1	154.9	769.3
0.0501	0.3441	0.0748	6.42	0.85	24.3	162.5	744.8
0.0628	0.4584	0.1269	6.98	0.80	23.6	186.9	705.6

5. Conclusion

Neutron star interiors are expected to contain extremely neutron rich nuclei (or more generally "nuclear structures", including those with unusual shapes), with neutron excess far beyond the laboratory neutron-drip limit. However, no stable nuclear structure can exist above a specific limiting density, which turns out to be significantly smaller than the saturation density of symmetric nuclear matter. For Skyrme forces SLy, which are particularly suitable for applications in neutron star matter calculations, this ultimate density is about 0.08 fm^{-3}, the proton fraction at the limiting density being about 4%.

The procedure of construction of SLy forces make them suitable also for the calculation of equation of state of neutron star matter at supranuclear densities, up to $8\rho_0$ [3]. Therefore these effective N–N interactions can be

used for a unified description of the whole neutron star, including its liquid interior. A low value of $\rho_{\rm max}^{\mathcal{N}}$ implies a small mass of neutron star crust. Consider a neutron star model of a "canonical mass" 1.4 $M_\odot$ (measured masses of binary radio pulsars are quite close to this canonical value). For SLy7 force, the mass of the crust constitutes then only 1.3% of stellar mass, while contribution of the crust to the total moment of inertia of neutron star is about 2.8% [12].

In spite of its small mass, the outer mantle of neutron star, containing neutron rich nuclei — neutron star crust — is of paramount importance for star evolution and dynamics. It insulates thermally neutron star surface from its liquid interior, and therefore plays an essential role in neutron star cooling. It can accumulate mechanical stresses, leading to instabilities crucial for the glitches in pulsar timing. Finally, neutron star crust can support, in contrast to the liquid interior, nonaxial deformations ("mountains") which, combined with rapid rotation, could make neutron star a source of continuous gravitational radiation. This gives a strong astrophysical motivation for theoretical studies of neutron rich nuclei in neutron star interiors.

We are grateful to G. Chabrier and J. Meyer for helpful remarks. P.H. acknowledges the hospitality of ENS de Lyon during his visit in the theoretical astrophysics group of CRAL. This work was supported in part by the KBN grant No. 2 P03D 014 13 and by the French CNRS/MAE program Jumelage Astronomie Pologne.

REFERENCES

[1] G. Baym, H.A. Bethe, C.J. Pethick, *Nucl. Phys.* **A175**, 225 (1971).

[2] M. Brack, B.K. Jennings, Y.H. Chu, *Phys. Lett.* **B65**, 1 (1976).

[3] E. Chabanat, P. Bonche, P. Haensel, J. Meyer, R. Schaeffer, *Nucl. Phys.*, **A627**, 710 (1997).

[4] E. Chabanat, P. Bonche, P. Haensel, J. Meyer, R. Schaeffer, *Nucl. Phys.* **A635**, 231 (1998).

[5] K.S. Cheng, C.C. Yao, Z.G. Dai, *Phys. Rev.* **C55**, 2092 (1997).

[6] K. Oyamatsu, *Nucl. Phys.* **A561**, 431 (1993).

[7] C.J. Pethick, A.Y. Potekhin, *Phys. Lett.* **B427**, 7 (1998).

[8] C.J. Pethick, D.G. Ravenhall, *Ann. Rev. Nucl. Part. Sci.* **45**, 429 (1995).

[9] C.P. Lorenz, D.G. Ravenhall, C.J. Pethick, *Phys. Rev. Lett.* **70**, 379 (1993).

[10] C.J. Pethick, D.G. Ravenhall, C.P. Lorenz, *Nucl. Phys.* **A584**, 675 (1995).

[11] K. Sumiyoshi, K. Oyamatsu, H. Toki, *Nucl. Phys.* **A595**, 327 (1995).

[12] F. Douchin, P. Haensel, submitted to *Phys. Lett.* **B** (1998).

[13] S.L. Shapiro, S.A. Teukolsky, *Black Holes, White Dwarfs and Neutron Stars*, Wiley, New York 1983, sect. 5.7.

[14] R.B. Wiringa, V. Fiks, A. Fabrocini, *Phys. Rev.* **C38**, 1010 (1988).

[15] F. Douchin, P. Haensel, to be submitted for publication.